HTML ABSTRACT + LINKS

Magnetization dependence on electron density in epitaxial ZnO thin films codoped with Mn and Sn

M. Ivill, S. J. Pearton, and D. P. Norton[a)]
Department of Materials Science and Engineering, University of Florida, Gainesville, Florida 32611-8440

J. Kelly and A. F. Hebard
Department of Physics, University of Florida, Gainesville, Florida, 32611-8440

(Received 3 September 2004; accepted 10 December 2004; published online 11 February 2005)

The magnetic and transport properties of Mn-doped ZnO thin films codoped with Sn are examined. Superconducting quantum interference device magnetometry measurements indicate that the films are ferromagnetic with an inverse correlation between magnetization and electron density as controlled by Sn doping. Magnetism in low free-electron density material is consistent with the bound magnetic polaron model, in which bound acceptors mediate the ferromagnetic ordering. Increasing the electron density decreases the acceptor concentration, thus quenching the ferromagnetic exchange. This result is important in understanding ferromagnetism in transition-metal-doped semiconductors for spintronic devices. © *2005 American Institute of Physics*. [DOI: 10.1063/1.1856225]

INTRODUCTION

The field of spintronics has attracted significant attention, most recently for its potential in providing functionality and enhanced performance in semiconducting devices, including spin-based field-effect transistors (FETs), spin-polarized lasers, light-emitting diodes (LEDs), nonvolatile magnetic semiconductor memory, and perhaps quantum computing.[1,2] Contemporary interest in dilute magnetic semiconductors[3–7] (DMSs) has been stimulated by the discovery of ferromagnetism in Mn-doped GaAs with a T_c of 110 K.[8] This value of Curie temperature is significantly higher than that observed in previously studied DMS materials. Nevertheless, the advancement of spintronics as a technology depends upon the development and understanding of semiconductors that can support spin-polarized carrier operation at or above room temperature.

Research efforts have identified several magnetically doped semiconductors that show evidence of ferromagnetic ordering above room temperature,[9–12] including transition-metal-doped ZnO. As a direct wide-band-gap material, ZnO is of interest for photonic, electronic, and magnetic applications.[13,14] Dietl *et al.* used Zener's model for ferromagnetism, driven by exchange interaction between hole charge carriers and localized spins, to predict ferromagnetism in *p*-type Mn-doped ZnO.[15] Motivated by this prediction, numerous studies have addressed the magnetic properties of transition-metal-doped ZnO with conflicting conclusions regarding magnetic behavior.[16–32] In particular, for Mn-doped ZnO, Jung *et al.*[21] reported low T_c (45 K) ferromagnetism, whereas Fukumura *et al.*[22] observed spin-glass behavior with a spin-freezing temperature of 13 K. For Mn doping, we have reported ferromagnetism with a Curie temperature approaching 250 K in Mn-implanted, Sn-doped bulk ZnO crystals.[23] High-temperature ferromagnetism was also reported in (Zn,Mn)O by Sharma *et al.* with a T_c above 425 K in bulk crystals and above 300 K in thin films.[12] With an apparent T_c above 300 K, Mn-doped ZnO is attractive for spintronic technology. Moreover, this material is useful in delineating the origin of ferromagnetism in a semiconductor host, primarily due to a lack of ferromagnetic secondary phases in the Zn–Mn–O phase diagram. For other transition-metal dopants, the possible presence of secondary ferromagnetic phases cannot be easily eliminated as the origin of the magnetic signals. For Mn-doped ZnO, the only ferromagnetic composition for this solid solution is Mn_3O_4, which is ferrimagnetic with a Curie temperature less than 50 K.[33,34] Therefore, any room-temperature ferromagnetism cannot be assigned to known secondary phases as none exist.

While experiments indicate high-temperature ferromagnetism in these materials, there remains some questions regarding the origin of the magnetic behavior in Mn-doped ZnO materials. The work of Dietl *et al.* predicted that highly *p*-type, Mn-doped ZnO should have Curie temperatures in excess of room temperature.[15,35,36] The theory assumes that ferromagnetic ordering between the localized moments of the Mn atoms is mediated by free holes in the material. While high hole concentrations are predicted to yield high Curie temperatures, carrier-mediated ferromagnetism in *n*-type material should be limited to lower temperatures. This distinction in carrier-type is attributed to the smaller density of states and exchange integral for Mn with the conduction band in comparison to the valence band,[37] as the Mn^{2+} state lies within the valence band of these materials. It is important to recognize that the exchange interaction for Mn, when placed in the wide-band-gap semiconductors, is fundamentally different from the other transition-metal ions. Mn *d* states lie in the valence band while the other transition-metal *d*-state orbitals introduce states within the gap. There are apparent discrepancies between the model and experimental results of Dietl *et al.* for Mn-doped ZnO. In these materials,

[a)]Author to whom correspondence should be addressed; FAX: 352-846-1182; electronic mail: dnort@mse.ufl.edu

 © 2005 American Institute of Physics

Downloaded 02 Aug 2006 to 128.227.24.18. Redistribution subject to AIP license or copyright, see http://jap.aip.org/jap/copyright.jsp

ferromagnetism has been reported in *n*-type and/or semi-insulating samples. In fact, achieving high hole carrier density in ZnO is a significant challenge that is being actively pursued for electronic applications.[38] An alternative model addresses whether ferromagnetic ordering of the Mn moments could originate from carriers (holes) that are present in the material, but localized at the transition-metal impurity.[39,40] The bound magnetic polaron model assumes an exchange interaction between the transition-metal (Mn) ion and localized (trapped) holes that are spatially near the Mn ion. As temperature decreases, the size of the bound magnetic polaron grows until its radius overlaps that of the neighboring polarons. This enables ferromagnetic ordering of the Mn ions in an otherwise insulating or semi-insulating material. Predictions based on this bound magnetic polaron model suggest that ferromagnetic ordering is possible. However, for Mn, it still depends on the availability of holes, albeit a localized distribution.

In this paper, we report on the synthesis and magnetic properties of Mn-doped ZnO epitaxial films that are codoped with Sn. Codoping allows independent control over the magnetic and electronic properties of the material by doping for each separately. In II-VI materials, the addition of Mn^{2+} does not introduce shallow donor states. By codoping II-VI semiconductors, Mn provides the localized spins needed for carrier-mediated ferromagnetism, with the additional dopant added to control the carrier concentration in the material. We investigated the carrier density dependence of saturation magnetization using Sn as a donor dopant.

EXPERIMENTS

Epitaxial Mn, Sn-doped ZnO films were grown by conventional pulsed-laser deposition. Laser ablation targets were prepared from high-purity powders of ZnO (99.999%), with MnO_2(99.999%) and SnO_2(99.95%) serving as the doping agents. The pressed targets were sintered at 1000 °C for 12 h in air. The targets were fabricated with a nominal composition of 3 at. % Mn and 0, 0.1, 0.01, and 0.001 at. % Sn. A Lambda Physik KrF excimer laser was used as the ablation source. The laser energy density was $1-3$ J/cm^2 with a laser repetition rate of 1 Hz and target-to-substrate distance of 6 cm. The growth chamber exhibits a base pressure of 10^{-5} Torr. Films were deposited onto single-crystal, *c*-plane oriented sapphire substrates. Film growth was conducted over a temperature range of 400–600 °C. An oxygen pressure of 20 mTorr was used for all film growth experiments. Film thicknesses were approximately 300–400 nm. X-ray diffraction was used to determine the crystallinity and secondary phase formation. Superconducting quantum interference device (SQUID) magnetometry was used to characterize the ferromagnetic behavior of the doped films, focusing on the films grown at 400 °C.

RESULTS

The phase stability and solid solubility of Mn in the ZnO films were investigated as a function of growth temperature for films with varying Sn concentrations. Figure 1 shows the x-ray diffraction scans for films deposited under the given

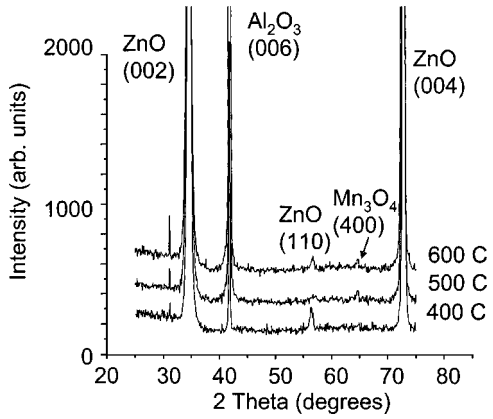

FIG. 1. X-ray diffraction of ZnO films codoped with Mn and Sn grown at an oxygen partial pressure of 20 mTorr and growth temperatures of 400, 500, and 600 °C. The target was ZnO doped with 3% Mn and 0.01% Sn.

growth conditions. In all cases, the dominant film peaks correspond to *c*-axis perpendicular ZnO. Note that, for some of the films, segregation of the Mn_3O_4 phase is evident in the diffraction data. As mentioned earlier, the Mn_3O_4 phase is ferromagnetic with a Curie temperature less than 50 K. The narrow peak located near 31° is an artifact peak from the sapphire substrate. Previous reports from Fukumura *et al.* indicated that epitaxial ZnO films with a Mn concentration as high as 35% could be achieved while maintaining the wurtzite structure using pulsed-laser deposition.[41] In this study, we find evidence for Mn oxide precipitation at a Mn concentration of only 3 at. % Mn, although the intensity of diffraction peaks from Mn_3O_4 varies with growth temperatures and Sn concentrations. This discrepancy between this work and that of Fukumura *et al.* might be attributed to the higher oxygen pressure used in our experiments (20 mTorr) as compared to 5×10^{-5} Torr in the experiments of Fukumura *et al.* Note that the precipitation of Sn-containing phases is not observed in the diffraction scan, nor is it expected even if present as the nominal concentration of Sn in the films is $\leqslant$0.1%.

The epitaxial nature of the ZnO films was determined using four-circle high-resolution x-ray diffraction. Figure 2(a) shows the x-ray diffraction ω scan about the ZnO (002) peak for the film grown on *c*-plane sapphire substrate at a growth temperature of 500 °C and Sn concentration of 0.1%. The ZnO (002) rocking curve displays a full width at half maximum (FWHM) of 0.5°. The in-plane alignment is evident in the phi scan of the ZnO (101) plane shown in Fig. 2(b). The phi-scan peaks at 60° intervals are consistent with the hexagonal symmetry of the epitaxial ZnO wurtzite structure.

The room-temperature resistivity for the Mn-doped ZnO films with varying concentrations of Sn was determined using a four-point van der Pauw geometry. Defect chemistry calculations for Mn-doped ZnO indicate that Mn^{+2} forms a donor level ~2.0 eV below the conduction-band edge.[42] This deep donor state with Mn substitution on the Zn site in ZnO has no direct effect on the electron concentration at room temperature. However, defect chemistry calculations also indicate a reduction in Zn interstitials with Mn doping. Zn interstitials are generally accepted as the primary shallow

Downloaded 02 Aug 2006 to 128.227.24.18. Redistribution subject to AIP license or copyright, see http://jap.aip.org/jap/copyright.jsp

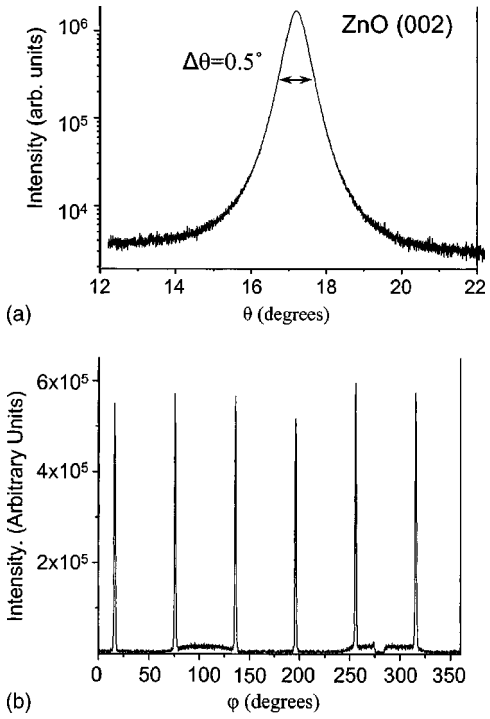

FIG. 2. X-ray diffraction of an epitaxial ZnO film doped with 3% Mn and 0.1% Sn that was deposited at 500 °C and $p(O_2)=20$ mTorr. (a) an ω-rocking curve of the ZnO (002) peak with a FWHM of 0.5°. (b) in-plane φ scan of the ZnO (101) planes.

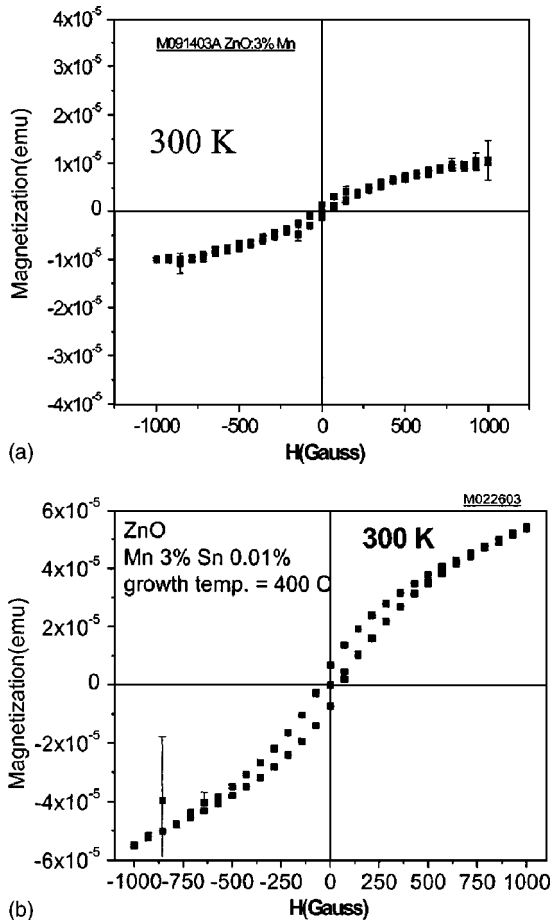

FIG. 3. SQUID measurements for epitaxial ZnO:3% Mn films without (a) and with (b) Sn codoping. Notice that the film without Sn exhibits little or no hysteresis, whereas the film with Sn shows hysteresis.

donor defects in nominally undoped ZnO. This will yield an increase in resistivity for Mn-doped films as compared to undoped material.[42–44] The Mn-doped ZnO films with no Sn exhibit a resistivity on the order of 10^2 Ω cm with a carrier density of mid-10^{16}/cm^3. This carrier density is substantially lower than that seen for undoped epitaxial films and is consistent with the reduction of shallow donors. Limited results on the doping behavior of Sn in ZnO indicate that it introduces a donor state,[45–49] although in some II-VI compound semiconductors, Sn is an amphoteric dopant, substituting on either the II or VI site.[50,51] For ZnO, the expectation is that Sn will substitute on the Zn site due to a close match in ionic radii between Zn^{+2} (0.074 nm) and Sn^{+4} (0.069 nm). For the epitaxial films considered in this work, Sn behaves as a donor. The resistivity of ZnO:Mn films with various Sn content is shown in Table I. The resistivity of the films drops rapidly with Sn doping with a minimum of 0.185 Ω cm for a Sn concentration of 0.1%. The most common valence state of Sn is +4, yielding a doubly ionized donor if doped substitutionally on the Zn site. Hall measurements indicate that the films are increasingly *n* type with Sn doping up to 0.1 at. %.

TABLE I. Resistivity as a function of Sn content in codoped ZnO:3% Mn films.

	% Sn concentration			
	0.0%	0.001%	0.01%	0.1%
Resistivity (Ω cm)	195	320	17	0.185

It should also be noted that other work has shown that the addition of Sn to ZnO ceramics also yields an enhancement in crystallinity.[45,46]

The magnetic properties of the films were measured using a Quantum Design SQUID magnetometer. The diamagnetic responses of the substrate and host semiconductor were subtracted from the magnetization plots. The primary focus of the measurements was to determine how the magnetic properties of the films changed as a function of electron density as controlled by Sn concentration. Samples that showed minimal amounts of Mn_3O_4 precipitation via x-ray diffraction were used for the SQUID measurements. Figure 3 shows the magnetization as a function of applied magnetic field for epitaxial ZnO:3% Mn films both without (a) and with (b) Sn codoping. For the Mn-doped film with no Sn, saturation in the magnetization is observed, but with little evidence for hysteresis in the *M* vs *H* curves. In contrast, the ZnO film doped with both Mn and Sn exhibits clear hysteresis. From the hysteresis curves, one can also observe an increase in loop width with increasing Sn concentration. Figure 4 shows the coercive field as a function of Sn concentration, suggesting domain pinning as the Sn doping is increased. It is unclear why the addition of Sn enhances the hysteretic magnetization response in the Mn-doped films. It might indicate enhanced pinning of domains due to the Sn dopants.

Downloaded 02 Aug 2006 to 128.227.24.18. Redistribution subject to AIP license or copyright, see http://jap.aip.org/jap/copyright.jsp

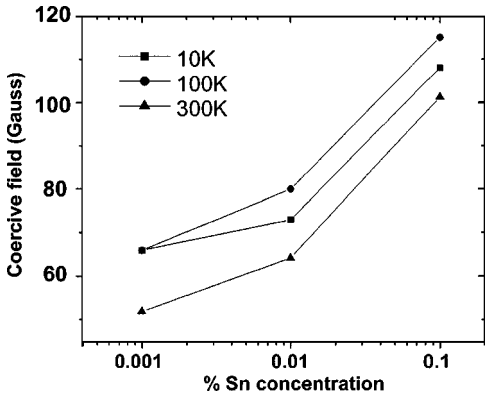

FIG. 4. A plot showing the dependence of the coercive field on Sn concentration at different SQUID measurement temperatures.

Most interesting is the saturation magnetization behavior as Sn content is increased. As noted earlier, increasing Sn concentration increases electron density and conductivity. Figure 5 shows the room-temperature magnetization versus field behavior for the ZnO samples containing 3% Mn and Sn contents of 0, 0.1, 0.01, and 0.001%. Magnetization is given as the magnetic-moment/Mn-dopant ion. Initially, there is an increase in magnetization with minimal Sn doping. However, with increasing Sn doping, there is an inverse correlation between the Sn content and saturation magnetization. As the electron density increases with Sn doping, the magnetization decreases. The maximum magnetization corresponds to a magnetic moment/Mn ion of ~0.5 bohr magnetons/Mn. This is consistent with the bound magnetic polaron model in which only a fraction of the Mn ions are expected to order ferromagnetically due to competing superexchange antiferromagnetic interactions between neighboring Mn ions.[52] The inverse correlation of saturation magnetization with electron density is interesting and provides some insight into the mechanism for ferromagnetism in Mn-doped ZnO. Overlap of the Mn *d* states with the valence band suggests that holes are necessary in order to induce ferromagnetic order. For semi-insulating films to exhibit ferromagnetism, the bound magnetic polaron model provides a mechanism whereby holes that are localized at or near the Mn ions are responsible for mediating ferromagnetism. The addition of electrons to the system will move the Fermi energy level up in the band gap, resulting in a decrease in hole density and a reduction in magnetization. This appears consistent with early work on trivalent-doped (Zn,Mn)O where no ferromagnetism was observed for heavily *n*-type films. It may also explain the discrepancy from other studies of Mn-doped ZnO films in which the intrinsic defect-mediated donor states are high in density. It is important to note the need to maintain a Mn concentration low enough to avoid Mn–Mn antiferromagnetic interactions, which are likely to dominate high Mn-doped ZnO films.

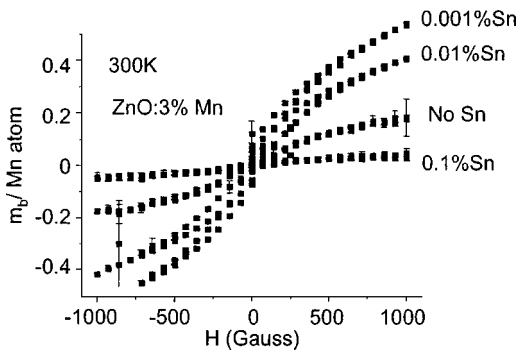

FIG. 5. Magnetization measured at 300 K for epitaxial ZnO:3% Mn films that are codoped with 0.001% Sn, 0.01% Sn, 0.1% Sn, and no Sn. There appears to be an inverse correlation of the Sn content with the saturation magnetization.

In conclusion, the magnetic and transport properties of Mn-doped ZnO thin films codoped with Sn were examined. Results indicate that the films are ferromagnetic with an inverse correlation between magnetization and electron density as controlled by Sn doping. The results are most consistent with the bound magnetic polaron model in which bound acceptors mediate the ferromagnetic ordering. Increasing the electron density decreases the acceptor concentration, thus quenching the ferromagnetic exchange. This result is relevant to understanding ferromagnetism in transition-metal-doped semiconductors.

ACKNOWLEDGMENTS

The work at UF is partially supported by AFOSR grant under Grant No. F49620-03-1-0370, by the Army Research Office under Grant No. DAAD19-01-1-0603, the Army Research Laboratory, AFOSR (Grant No. F49620-02-1-0366, G. Witt), NSF (Grant No. CTS-0301178, monitored by Dr. M. Burka and Dr. D. Senich), by NASA Kennedy Space Center Grant No. NAG 10-316 monitored by Mr. Daniel E. Fitch, and the National Science Foundation (Grant No. DMR 0400416, 0101856). The authors would like to acknowledge the Major Analytical Instrumentation Center, Department of Materials Science and Engineering, University of Florida.

[1] S. A. Wolf, D. D. Awschalom, R. A. Buhrman, J. M. Daughton, S. von Molnár, M. L. Roukes, A. Y. Chtchelkanova, and D. M. Treger, Science **294**, 1488 (2001).
[2] G. A. Prinz, Science **282**, 1660 (1998).
[3] J. K. Furdyna, J. Appl. Phys. **64**, R29 (1988).
[4] S. Gopalan and M. G. Cottam, Phys. Rev. B **42**, 10311 (1990).
[5] C. Haas, CRC Crit. Rev. Solid State Sci. **1**, 47 (1970).
[6] T. Suski, J. Igalson, and T. Story, J. Magn. Magn. Mater. **66**, 325 (1987).
[7] A. Haury, A. Wasiela, A. Arnoult, J. Cibert, S. Tatarenko, T. Dietl, and Y. Merle d'Aubigne, Phys. Rev. Lett. **79**, 511 (1997); P. Kossacki *et al.*, Physica E (Amsterdam) **6**, 709 (2000).
[8] H. Ohno, Science **281**, 951 (1998).
[9] S. J. Pearton, C. R. Abernathy, D. P. Norton, A. F. Hebard, Y. D. Park, L. A. Boatner, and J. D. Budai, Mater. Sci. Eng., R. **40**, 137 (2003).
[10] M. Ivill, M. E. Overberg, C. R. Abernathy, D. P. Norton, A. F. Hebard, N. Theodoropoulou, and J. D. Budai, Solid-State Electron. **47**, 2215 (2003).
[11] Y. Matsumoto *et al.*, Science **291**, 854 (2001).
[12] P. Sharma *et al.*, Nat. Mater. **2**, 673 (2003).
[13] D. C. Look, Mater. Sci. Eng., B **80**, 383 (2001).
[14] S. Masuda, K. Kitamura, Y. Okumura, S. Miyatake, H. Tabata, and T. Kawai, J. Appl. Phys. **93**, 1624 (2003).
[15] T. Dietl, H. Ohno, F. Matsukura, J. Cubert, and D. Ferrand, Science **287**, 1019 (2000).
[16] K. Sato and H. Katayama-Yoshida, Jpn. J. Appl. Phys., Part 2 **39**, L555 (2000).
[17] J. H. Kim, H. Kim, D. Kim, Y. E. Ihm, and W. K. Choo, J. Appl. Phys. **92**, 6066 (2002).
[18] H.-J. Lee, S.-Y. Jeong, C. R. Cho, and C. H. Park, Appl. Phys. Lett. **81**, 4020 (2002).
[19] T. Wakano, N. Fujimura, Y. Morinaga, N. Abe, A. Ashida, and T. Ito,

Downloaded 02 Aug 2006 to 128.227.24.18. Redistribution subject to AIP license or copyright, see http://jap.aip.org/jap/copyright.jsp

Physica E (Amsterdam) **10**, 260 (2001).
[20]S.-J. Han, J. W. Song, C.-H. Yang, S. H. Park, J.-H. Park, Y. H. Jeong, and K. W. Rhie, Appl. Phys. Lett. **81**, 4212 (2002).
[21]S. W. Jung, S.-J. An, G.-C. Yi, C. U. Jung, S.-I. Lee, and S. Cho, Appl. Phys. Lett. **80**, 4561 (2002).
[22]T. Fukumura, Z. Jin, M. Kawasaki, T. Shono, T. Hasegawa, S. Koshihara, and H. Koinuma, Appl. Phys. Lett. **78**, 958 (2001).
[23]D. P. Norton, S. J. Pearton, A. F. Hebard, N. Theodoropoulou, L. A. Boatner, and R. G. Wilson, Appl. Phys. Lett. **82**, 239 (2003).
[24]M. S. Park and B. I. Min, Phys. Rev. B **68**, 224436 (2003).
[25]Y. Q. Chang *et al.*, Appl. Phys. Lett. **83**, 4020 (2003).
[26]A. S. Risbud, N. A. Spaldin, Z. Q. Chen, S. Stemmer, and R. Seshadri, Phys. Rev. B **68**, 205202 (2003).
[27]S.-J. Han, T.-H. Jang, Y. B. Kim, B.-G. Park, J.-H. Park, and Y. H. Jeong, Appl. Phys. Lett. **83**, 920 (2003).
[28]S. W. Yoon, S.-B. Cho, S. C. We, S. Yoon, B. J. Suh, H. K. Song, and Y. J. Shin, J. Appl. Phys. **93**, 7879(2003).
[29]V. A. L. Roy *et al.*, Appl. Phys. Lett. **84**, 756 (2004).
[30]X. M. Cheng and C. L. Chien, J. Appl. Phys. **93**, 7876 (2003).
[31]S. S. Kim, J. H. Moon, B.-T. Lee, O. S. Song, and J. H. Je, J. Appl. Phys. **95**, 454 (2004).
[32]S. Kolesnik, B. Dabrowski, and J. Mais, J. Appl. Phys. **95**, 2582 (2004).
[33]L. W. Guo, D. L. Peng, H. Makino, K. Inaba, H. J. Ko, K. Sumiyama, and Y. Yao, J. Magn. Magn. Mater. **213**, 321 (2000).
[34]A. Chartier, P. D'Arco, R. Dovesi and V. R. Saunders, Phys. Rev. B **60**, 14042 (1999).
[35]T. Dietl, A. Haury, and Y. Merle d'Aubigne, Phys. Rev. B **55**, R3347 (1997).
[36]T. Dietl, Semicond. Sci. Technol. **17**, 377 (2002).
[37]H. Ohno, *Ferromagnetic III-V Semiconductors and Their Heterostructures*, Semiconductor Spintronics and Quantum Computation, edited by D. D. Awschalom, D. Loss, and N. Samarth (Springer, New York, 2002), Chap. 1.
[38]D. C. Look, D. C. Reynolds, C. W. Litton, R. L. Jones, D. B. Eason, and G. Cantwell, Appl. Phys. Lett. **81**, 1830 (2002).
[39]A. Kaminski and S. Das Sarma, Phys. Rev. Lett. **88**, 247202 (2002).
[40]M. Berciu and R. N. Bhatt, Phys. Rev. Lett. **87**, 107203 (2001).
[41]T. Fukumura, Z. Jin, A. Ohtomo, H. Koinuma, and M. Kawasaki, Appl. Phys. Lett. **75**, 3366 (1999).
[42]J. Han, P. Q. Mantas, and A. M. R. Senos, J. Eur. Ceram. Soc. **22**, 49 (2002).
[43]Z. Zhou, K. Kato, T. Komaki, M. Yoshino, H. Yukawa, M. Morinaga, and K. Morita, J. Eur. Ceram. Soc. **24**, 139 (2004).
[44]N. Ohashi, J. Tanaka, T. Ohgaki, H. Haneda, M. Ozawa, and T. Tsurumi, J. Mater. Res. **17**, 1529 (2002).
[45]F. Paraguay, J. Morales, W. Estrada, E. Andrade, and M. Miki-Yoshida, Thin Solid Films **366**, 16 (2000).
[46]A. Bougrine, A. El. Hichou, M. Addou, J. Ebothé, A. Kachouane, and M. Troyon, Mater. Chem. Phys. **80**, 438 (2003).
[47]J.-H. Lee and B.-O. Park, Thin Solid Films **426**, 94 (2003).
[48]H. Sato, T. Minami, and S. Takata, J. Vac. Sci. Technol. A **11**, 2975 (1993).
[49]E. Holmelund, J. Schou, S. Tougaard, and N. B. Larsen, Appl. Surf. Sci. **197**, 467 (2002).
[50]I. Turkevych, R. Grill, J. Franc, P. Höschl, E. Belas, and P. Moravec, Cryst. Res. Technol. **38**, 288 (2003).
[51]O. Panchuk *et al.*, J. Cryst. Growth **197**, 607 (1999).
[52]T. Dietl *et al.*, Phys. Status Solidi B **229**, 665 (2002).

Downloaded 02 Aug 2006 to 128.227.24.18. Redistribution subject to AIP license or copyright, see http://jap.aip.org/jap/copyright.jsp